THE ASTROPHYSICAL JOURNAL, 417:815–825, 1993 November 10

CONDENSATION AND VAPORIZATION STUDIES OF CH_3OH AND NH_3 ICES: MAJOR IMPLICATIONS FOR ASTROCHEMISTRY

SCOTT A. SANDFORD AND LOUIS J. ALLAMANDOLA
NASA/Ames Research Center, Mail Stop 245-6, Moffett Field, CA 94035
Received 1993 March 5; accepted 1993 May 17

ABSTRACT

In an extension of previously reported work on ices containing H_2O, CO, CO_2, SO_2, H_2S, and H_2, we present measurements of the physical and infrared spectral properties of ices containing CH_3OH and NH_3. The condensation and sublimation behavior of these ice systems is discussed and surface binding energies are presented for all of these molecules. The surface binding energies can be used to calculate the residence times of the molecules on grain surfaces as a function of temperature. It is demonstrated that many of the molecules used to generate radio maps of and probe conditions in dense clouds, for example CO and NH_3, will be significantly depleted from the gas phase by condensation onto dust grains. Attempts to derive total column densities solely from radio maps that do not take condensation effects into account may vastly underestimate the true column densities of any given species. Simple CO condensation onto and vaporization off of grains appears to be capable of explaining the observed depletion of gas phase CO in cold, dense molecular cores. This is not the case for NH_3, however, where thermal considerations alone predict that *all* of the NH_3 should be condensed onto grains. The fact that some gas phase NH_3 *is* observed indicates that additional desorption processes must be involved. The surface binding energies of CH_3OH, in conjunction with this molecule's observed behavior during warm up in H_2O-rich ices, is shown to provide an explanation of the large excess of CH_3OH seen in many warm, dense molecular cores. The near-infrared spectrum and associated integrated band strengths of CH_3OH-containing ice are given, as are middle infrared absorption band strengths for both CH_3OH and NH_3.

Subject headings: dust, extinction — molecular processes

1. INTRODUCTION

In several previous papers, laboratory studies of the condensation and vaporization properties of ice systems containing CO, CO_2, and H_2O (Sandford & Allamandola 1988, 1990a, b), SO_2, H_2S, and CO_2 (Sandford & Allamandola 1993a), and H_2 (Sandford & Allamandola 1993b) were reported. Surface binding energies (ΔH_s) were determined for each of the molecular components in these ices. Surface binding energies can be used to calculate molecular residence times on an ice surface as a function of temperature and can therefore be used to derive sublimation rates. These rates provide a measure of the ice's thermal stability with respect to sublimation. There are a number of astrophysical environments where an understanding of an ice's sublimation behavior and thermal stability is clearly important. These include dense molecular clouds, cometary nuclei and comae, and the surfaces and atmospheres of some planets and satellites.

In this contribution, the results of surface binding energy measurements of ice systems containing CH_3OH and NH_3 are given. The techniques used to measure the binding energies are discussed in § 2. The results of these and earlier binding energy studies are summarized in § 3. In addition, § 3 also reports new measurements of some spectral properties (band positions, widths, and strengths) of NH_3 and CH_3OH ices. In § 4, some of the more important astrophysical implications are discussed. The conclusions are then summarized in § 5.

2. TECHNIQUE AND RESULTS

Only a brief summary of the experimental procedures used is given here since a detailed description of the equipment and techniques has already been presented elsewhere (Allamandola, Sandford, & Valero 1988; Sandford & Allamandola 1988, 1990a, 1993a).

2.1. *Deposition and Sublimation Techniques*

All the gas mixtures used in these studies were prepared in a greaseless, glass vacuum system designed to allow for careful control of molecular concentrations. All liquids used (H_2O and CH_3OH, J. T. Baker photorex grade purity >99.9%) were further purified by three freeze-thaw cycles under vacuum before they were used as gas sources. CO and NH_3 (purity >99.5%) were taken directly from Matheson gas cylinders and used without further purification.

After allowing ample time for mixing of the gases in each bulb, the gas samples were condensed onto a cold CsI window suspended in a vacuum chamber. Depositions were made at pressures of $\sim 3 \times 10^{-8}$ mb. The flow of gas onto the CsI window was regulated by a microflowmeter and samples were typically deposited at rates of $\sim 1.5 \times 10^{-5}$ mol hr^{-1}, corresponding to a thickness growth rate of ~ 5 μm hr^{-1}. The window was cooled by a closed-cycle helium refrigerator whose temperature could be maintained at any point between 10 and 280 K by a resistive heater. The temperature was measured with an absolute accuracy of ± 2 K and a relative accuracy of ± 0.2 K with an Fe-Au/Chromel thermocouple placed inside the window holder. The CsI window can be rotated, without breaking the vacuum, to line up with the beam axis of a Fourier transform infrared spectrometer.

2.2. *Infrared Spectroscopy Techniques*

Infrared transmission spectra were measured from 7000 to 400 cm^{-1} (1.4–25 μm) at a resolution of 0.9 cm^{-1} (the

observed width of an unresolved line). Spectral positions are accurate to ± 0.2 cm^{-1} because of oversampling. The amounts of material in the ice samples were monitored by measuring the absorption band areas of characteristic vibrational modes of each molecule (see Table 1). The column density of molecules in the infrared beam can then be easily derived using the equation

$$N_i = \frac{\int \tau(\nu) d\nu}{A_i}, \quad (1)$$

where N_i is the column density of component i in molecules cm^{-2}, $\tau(\nu)$ is the optical depth of the absorption band as a function of frequency, and A_i is the integrated absorbance of the appropriate band in cm molecule^{-1}.

2.3. *Derivation of Binding Energies*

The surface binding energies of molecules in pure, one-component ices can be determined in a straightforward fashion by measuring the rate at which the ice sublimes as a function of temperature (Sandford & Allamandola 1988, 1990a). This technique is based on the assumption that the deposition-sublimation behavior of the ices is described by the models of Langmuir (1916) and Frenkel (1924) in which it is assumed that the sticking efficiency of a deposited molecule is equal to 1.0 and that escape from the surface (reevaporation) takes place at a rate given by

$$R_s = \nu_0 \exp(-\Delta H_s/kT), \quad (2)$$

where ν_0 is the lattice vibrational frequency of the molecule within its surface matrix site, ΔH_s is the binding energy of the molecule on the ice surface, k is the Boltzmann constant, and T is the ice temperature in kelvins.

The surface binding energy of molecules in a single component ice can be found by depositing the ice at a low temperature (typically 10 K), warming the ice to a predetermined temperature, and holding it there while the loss of ice by sublimation is monitored by following the decrease in strength of an infrared absorption feature as a function of time. We will use the common formalism of expressing binding energies in terms of $(\Delta H/k)$, i.e., in kelvins throughout this paper. The measured loss of material can then be used to calculate the binding energy from the equation

$$\frac{\Delta H_s}{k} = -T \ln\left\{\frac{a_m}{\nu_0 t_f A}[(\tau\Delta\nu)_i - (\tau\Delta\nu)_f]\right\}, \quad (3)$$

where a_m is the area of the molecular site on the ice surface, t_f is the time span over which the loss is measured, $(\tau\Delta\nu)_i$ is the integrated band strength of the infrared absorption feature at time $t_i = 0$, $(\tau\Delta\nu)_f$ is the integrated band strength at time t_f, and A is the integrated absorbance of the spectral feature being monitored in cm molecule^{-1} (see Sandford & Allamandola 1988, 1990a for a more complete discussion). This technique works best when the loss rate is measured at several temperatures near the point at which the ice loss rate is in the range of microns per hour.

3. EXPERIMENTAL RESULTS

The ice systems discussed below were chosen for study because their condensation and sublimation properties are likely to be important in several astrophysical environments,

TABLE 1

BAND POSITIONS AND A VALUES FOR THE ABSORPTION BANDS ASSOCIATED WITH THIS WORK[a]

Molecule	Mode	Position (cm^{-1})	A-Value (cm per molecule)	Source Reference
CH_3OH	$2\nu_3$	5660	1×10^{-19} [b]	1
	$(\nu_1 + \nu_{11})$ or $(\nu_1 + \nu_7)$	4404	4×10^{-19} [b]	1
	$(\nu_1 + \nu_8)$	4277	6×10^{-20} [b]	1
	$(\nu_2 + \nu_7)$ or $(\nu_2 + \nu_{11})$	4132	2×10^{-20} [b]	1
	$(\nu_2 + \nu_8)$, $(\nu_8 + \nu_9)$, $(2\nu_4, \nu_{10} + \nu_8)$	4020, 3990, 3950	1.4×10^{-19} [b]	1
	$(\nu_3 + \nu_8)$	3856	2×10^{-20} [b,c]	1
	OH and CH stretch	3251, 2951, 2827	1.6×10^{-18}	2
	ν_1 OH stretch	3251	1.3×10^{-16}	2
	ν_9 and ν_3 CH stretch	2951, 2827	2.6×10^{-17}	2
	ν_9 CH stretch	2951	2.1×10^{-17}	2
	ν_3 CH stretch	2827	5.3×10^{-18}	2
	Combinations	2600, 2526	2.6×10^{-18}	3
	ν_4, ν_5, ν_6, ν_{10} CH_3 deformation	"1460"	1.2×10^{-17}	2
	ν_7, ν_{11} CH_3 rock	1130	1.8×10^{-18} [d]	2
	ν_8 CO stretch	1026	1.8×10^{-17}	4
	ν_{12} torsion	694	1.4×10^{-17}	2
NH_3	(ν_1, ν_3) NH stretch	3375	2.2×10^{-17}	4
	ν_4 NH deformation	1624	4.7×10^{-18}	1
	ν_2 umbrella mode	1070	1.7×10^{-17}	4

[a] For a more complete list of A-values for many molecules of astrophysical interest, see d'Hendecourt & Allamandola 1986 and Hudgins et al. 1993.

[b] Valid when the CH_3OH is in an H_2O-rich matrix.

[c] Valid at 10 K. Value increases by about 6% per 10 K upon warm-up.

[d] Valid for pure CH_3OH. When the CH_3OH is in an H_2O-rich matrix, a value of 2.4×10^{-18} cm per molecule is appropriate.

REFERENCES.—(1) This work. The vibrational assignments of the CH_3OH overtone/combination bands are tentative and are based solely on frequency proximities; (2) Hudgins et al. 1993; (3) Allamandola et al. 1992; (4) d'Hendecourt & Allamandola 1986.

including dense molecular clouds, comets, and the surfaces and atmospheres of some planets and satellites. The discussion will focus on applications associated with dense molecular clouds.

3.1. *The* CH_3OH-CH_3OH *Surface Binding Energy*

Methanol (CH_3OH) is now known to be the second most abundant molecule in many interstellar ices (typically 5%–50% that of H_2O), and it has been identified by its characteristic absorption bands at 2825 cm^{-1} (3.54 μm; Grim et al. 1991, Allamandola et al. 1992), 2600 and 2540 cm^{-1} (3.85 and 3.94 μm; Allamandola et al. 1992), 1460 cm^{-1} (6.85 μm; Tielens & Allamandola 1987), and 1128 and 1026 cm^{-1} (8.9 and 9.7 μm; Skinner et al. 1992). Indeed, in terms of the total number of absorption features detected, the CH_3OH identification is firmer than that of H_2O! Methanol has also been detected in comets at abundances up to 6% relative to H_2O (Hoban et al. 1991; Reuter 1992).

The presence of methanol in interstellar and cometary ices has important implications for both their physical and chemical properties. For example, amorphous H_2O:CH_3OH ices spontaneously form a type II clathrate structure in a vacuum when heated to $\sim$125 K if the methanol concentration is greater than $\sim$6% (Blake et al. 1991). If the CH_3OH concentration is >7%, the mixed molecular ice undergoes clathrate formation and a phase separation that excludes excess methanol, resulting in an ice containing intermingled crystals of H_2O:CH_3OH clathrate and pure CH_3OH ice. The significance of this finding with regard to the large gas phase CH_3OH abundances found in hot molecular cores (cf. Walmsley 1989) will be discussed in more detail in § 4.

Methanol is also important because its presence drives a rich UV photochemistry that produces a multitude of new compounds, including some relatively complex organic materials (Allamandola et al. 1988; Sandford et al. 1991). Because of its large solid state abundance and its effect on the physical and chemical properties of the ices, the sublimation and condensation properties of CH_3OH ices are of central importance.

The CH_3OH-CH_3OH surface binding energy was determined using equation (3) and the experimental techniques discussed in §§ 2.1–2.3. Two different experiments were done. In each experiment, pure CH_3OH was deposited at 10 K. The resulting ices were then warmed at 2 K per minute to temperatures of 140 and 144 K, respectively. Both ices were then allowed to equilibrate for 10 minutes before measurements of the sublimation rate were begun. A plot of the CH_3OH loss from these ices as a function of time and temperature is given in Figure 1.

The amount of CH_3OH in the infrared beam was determined by measuring the integrated area of the ν_8 C—O stretch band near 1026 cm^{-1} (see Fig. 2) and using equation (1). The absorbance strength used for the ν_8 band is given in Table 1. A value of $\nu_0 = 2.2 \times 10^{12}$ sec^{-1} was determined from the infrared spectra of CH_3OH in hydroquinone and argon matrices which show lattice modes at 73 and 70 cm^{-1}, respectively (Barthel, Gerbaux, & Hadni 1970; Passchier 1978). The group dimensions of α-phase CH_3OH at 113 K are reported to be $a = 4.53$ Å, $b = 4.69$ Å, and $c = 4.91$ Å (Schudt & Weitz 1971). This corresponds to an average unit cell side dimension of 4.71 Å which implies an average molecular surface site area of 1.40×10^{15}, since there are two CH_3OH per cell.

Using equation (3), the parameter values given above, and the data presented in Figure 1, we measured multiple values of the CH_3OH-CH_3OH surface binding energy for both the 140 and 144 K ices. Considering the entire data set, a final CH_3OH-CH_3OH surface binding energy of $\Delta H_s/k = 4235 \pm 15$ K was obtained.

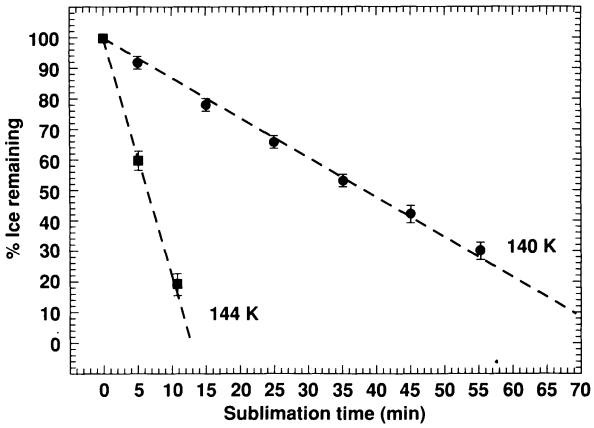

FIG. 1.—The loss of CH_3OH from a pure CH_3OH ice as a function of time for ices at 140 and 144 K. Both ices were deposited at 10 K and warmed to the indicated temperatures at a rate of 2 K per minute.

3.2. *Infrared Band Strengths for* CH_3OH

While the infrared spectra of dense molecular clouds demonstrate that methanol is an abundant component of interstellar ices, the exact proportion of CH_3OH to H_2O remains uncertain. The strength of the 1460 cm^{-1} (6.85 μm) methanol band suggests that many clouds contain high CH_3OH/H_2O ratios (0.4–0.6; cf. Tielens & Allamandola 1987), while the strength of the 2825 cm^{-1} (3.54 μm) band in some of the same objects suggests lower ratios (0.05–0.20: Grim et al. 1991; Allamandola et al. 1992). This discrepancy may be due to one or more of several effects. One possibility is that some of the absorption at 1460 cm^{-1} is due to the presence of another material. Alternatively, the strength of the 2825 cm^{-1} band may be underestimated due to confusion associated with its baseline (the feature falls on the low-frequency wing of the strong O—H stretching feature of H_2O). Finally, it is possible that the discrepancy could be due to scattering effects associated with the embedded infrared sources themselves (Allamandola et al. 1992).

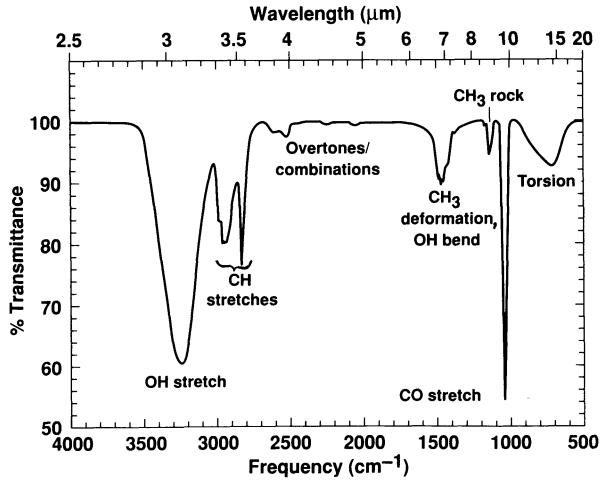

FIG. 2.—The 4000–500 cm^{-1} (2.5–20 μm) spectrum of a pure CH_3OH ice deposited at 10 K.

This abundance issue is a critical one to resolve because of the physical and chemical importance of CH_3OH. One approach is to search for other infrared bands due to methanol which avoid the above complications, measure their strength, and use equation (1) to derive additional column densities for comparison. We have therefore extended our spectral study to include many of the overtone/combination bands produced in the 6000–3700 cm^{-1} spectral region by CH_3OH in H_2O-rich ices.

The 6000–3700 cm^{-1} spectrum of an $H_2O:CH_3OH = 2:1$ ice contains CH_3OH bands at 5660, 4404, 4277, 4132, 4020, 3990, 3950, and 3856 cm^{-1}. The 4550–3750 cm^{-1} region is shown in Figure 3. Absorbance strengths (A-values) were determined for these bands by dividing the integrated band area (in absorbance) of each feature with the integrated band area of the ν_8 CO stretch band at 1026 cm^{-1} and multiplying by the A-value of the 1026 cm^{-1} band ($A_{1026} = 1.8 \times 10^{-17}$ cm per molecule; d'Hendecourt & Allamandola 1986). This was done for a large number ($N > 34$ for all bands) of independently deposited ices. The derived band strengths and tentative identifications of the overtone/combination vibrational modes responsible are given in Table 1.

3.3. *The* NH_3-NH_3 *Surface Binding Energy*

Much of our knowledge of the conditions in dense molecular clouds and their cores comes from radio observations of NH_3 (see, for example, Fuller & Myers 1987 for a review). From the study of different rotation lines of this molecule, it is possible to derive model dependent information about cloud core densities, rotation, magnetic fields, etc. Of course, the nature of these observations restricts them to NH_3 in the gas phase. As a result, it is not uncommon in the application of these techniques to ignore the effect that solid grains may have on the behavior and composition of the gas. This can lead to severe conceptual inconsistencies since the low-temperature dust grains can act as an important source/sink for the gas. There is some evidence that NH_3 is present in interstellar ices (Hagen, Allamandola, & Greenberg 1980; Knacke et al. 1982; Eiroa & Hodapp 1989), although it has not yet been unequivocally detected.

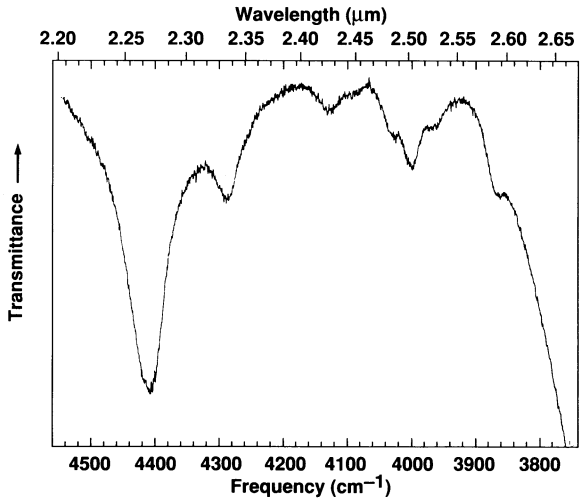

FIG. 3.—The 4550–3750 cm^{-1} (2.20–2.67 μm) spectrum of an $H_2O:CH_3OH = 2:1$ ice at 10 K. The absorption bands are due to overtones and combinations of lower frequency fundamental modes of methanol. See the text and Table 1 for further discussion.

The abundance and physical behavior of ammonia is also of interest since this molecule is expected to be an important carrier of cosmic nitrogen and is likely to be important in many interstellar reactions associated with nitrogen chemistry (cf. Tielens & Hagen 1982; Nejad, Williams, & Charnley 1990). In addition, in many astrophysical environments frozen NH_3 may act as a catalyst as well as a reactant (Schutte, Allamandola, & Sandford 1993a, b). Thus, it is clear that the sublimation properties of NH_3 ices are of interest to a variety of astrophysical problems.

The NH_3-NH_3 surface binding energy was derived in the same manner as for CH_3OH. Three different experiments were done. In each experiment, pure NH_3 was deposited at 10 K. The resulting ices were then warmed at 2 K per minute to temperatures of 100, 103, and 105 K, respectively. The ices were then allowed to equilibrate for 10 minutes before measurements of the sublimation rate were begun. The amount of NH_3 in the infrared beam was determined by monitoring the ν_4 NH deformation band near 1624 cm^{-1} and the ν_2 umbrella mode near 1070 cm^{-1} (see Fig. 4). The $(\nu_1 + \nu_3)$ N—H stretch band near 3375 cm^{-1} was not used because it exhibits a broad, low-frequency wing which makes it difficult to reliably determine the feature's true strength. The A-values used for the 1624 and 1070 cm^{-1} bands are given in Table 1.

A plot of the NH_3 loss from these ices as a function of time and temperature is given in Figure 5. Spectra of solid NH_3 show far-infrared absorption bands at approximately 140 and 80 cm^{-1} (Sill, Fink, & Ferraro 1980). Assuming these are lattice modes, we derive an average lattice mode frequency of 115 cm^{-1}. This corresponds to a value of $\nu_0 = 3.45 \times 10^{12}$ s^{-1}. Landolt-Bornstein (1978) gives a unit cell dimension of $a = 5.084$ Å for a 77 K NH_3 ice. Jones (1973) reports a dimension of $a = 5.084$ Å at 77 K and four NH_3 per cell. Assuming an average cell side dimension of 5.10 Å, we find an average molecular surface site area of 1.02×10^{-15} cm^2.

Using equation (3), the parameters given above, and the data presented in Figure 5, we calculated an NH_3-NH_3 surface binding energy for each of the ices. For the 100 K ice we determined values of $\Delta H_s/k = 3059$ K and 3054 K from the 1624 and 1070 cm^{-1} bands, respectively. Similarly, for the 103 K ice we determined values of 3095 K and 3085 K, and for the 105 K ice we determined values of 3087 K and 3083 K. Averag-

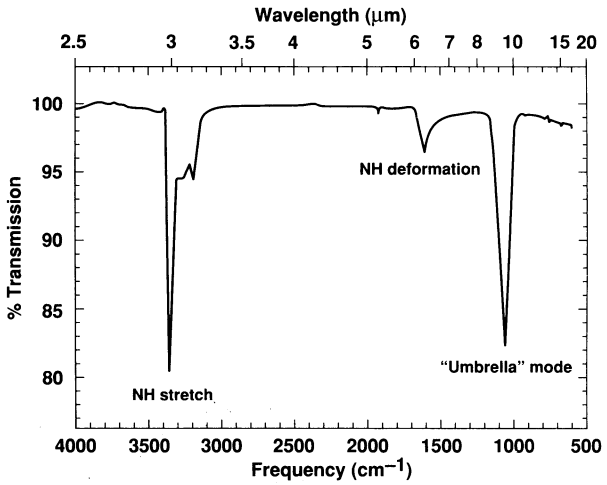

FIG. 4.—The 4000–500 cm^{-1} (2.5–20.0 μm) spectrum of a pure NH_3 ice deposited at 10 K.

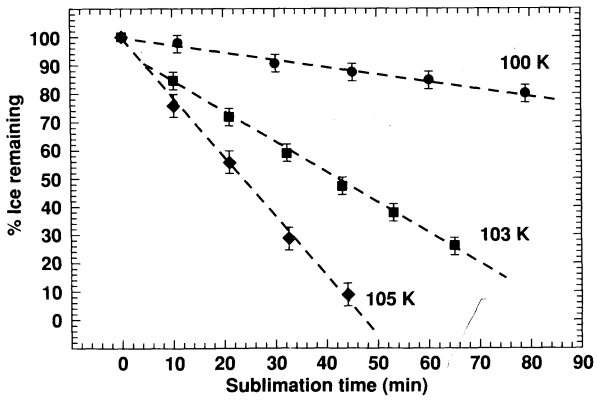

FIG. 5.—The loss of NH_3 from a pure NH_3 ice as a function of time for ices at 100, 103, and 105 K. All three ices were deposited at 10 K and warmed to the indicated temperatures at a rate of 2 K per minute.

ing the entire data set, a final NH_3-NH_3 surface binding energy of $\Delta H_s/k = 3075 \pm 25$ K is derived.

3.4. *Infrared Band Strengths for* NH_3

The absorption coefficients for the ν_1 and ν_3 N—H stretch and ν_2 "umbrella" mode bands of pure NH_3 ice have been reported by d'Hendecourt & Allamandola (1986). We have determined the integrated absorbance strength (A-value) of the ν_4 NH deformation vibration near 1624 cm^{-1} by dividing the integrated band area (in absorbance) of this feature by the integrated band area of the ν_2 umbrella mode at 1070 cm^{-1} and multiplying by the A-value of the 1070 cm^{-1} band. This was done for 10 independently deposited pure NH_3 ices and the results averaged. We find a value of $A_{1624} = 4.7 \times 10^{-18}$ cm per molecule for pure solid NH_3. A summary of the NH_3 results can be found in Table 1.

3.5. *Systems Containing Other Molecules*

The surface and volume binding energies of ice systems containing H_2O, CO, CO_2, SO_2, H_2S, and H_2 are also expected to be of use for the modeling of various astrophysical environments. More complete discussions of ice systems containing CO, CO_2, H_2O, and H_2 (appropriate for many interstellar, cometary, and planetary ices) can be found in Sandford & Allamandola (1988, 1990a, b, 1993b). A similar discussion concerning ices containing SO_2, H_2S, and CO_2 (appropriate for Jupiter's moon Io) can be found in Sandford & Allamandola (1993a). A complete summary of the binding energy results presented here and those published earlier can be found in Tables 2 and 3.

TABLE 2

THE SURFACE BINDING ENERGIES OF ASTROPHYSICALLY RELEVANT ICES

Ice System	Ice Sample	Surface Binding Energy ($\Delta H_s/k$) (K)
CH_3OH on CH_3OH[a]	Pure CH_3OH	4235±15
NH_3 on NH_3[a]	Pure NH_3	3075±25
CO on CO[b]	Pure CO	960±10
CO_2 on CO_2[c]	Pure CO_2	2690±150
CO on H_2O[c]	H_2O:CO = 20:1	1740±50
CO_2 on H_2O[c]	H_2O:CO_2 = 20:1	2860±150
H_2O on H_2O[b]	Unannealed pure H_2O	4815±15
	Annealed pure H_2O	5070±50
SO_2 on SO_2[d]	Pure SO_2	3460±40
CO_2 on SO_2[d]	SO_2:CO_2 = 20:1	2235±50
H_2S on SO_2[d]	SO_2:H_2S = 20:1	1945±125
H_2 on H_2O:CH_3OH[e]	H_2O:CH_3OH:H_2 = 10:5:1	555±35
H_2 on H_2[f]	Pure H_2	~100
H on H_2O[g]	...	450

[a] This work.
[b] Taken from Sandford & Allamandola 1988.
[c] Taken from Sandford & Allamandola 1990a.
[d] Taken from Sandford & Allamandola 1993a.
[e] Taken from Sandford & Allamandola 1993b.
[f] Taken from Brown & Ziegler 1980 and Souers 1986.
[g] Calculation from Hollenbach & Salpeter 1970.

4. ASTROPHYSICAL IMPLICATIONS

It has long been realized that most gas phase molecules in dense molecular clouds should freeze out onto grains within a few hundred years (cf. van de Hulst 1949; Greenberg 1977;

TABLE 3

COMPARISON OF THE RESIDENCE TIMES OF SOME ASTROPHYSICALLY RELEVANT MOLECULES ON VARIOUS ICES AS A FUNCTION OF ICE TEMPERATURE[a]

T (K)	CH_3OH on CH_3OH	NH_3 on NH_3	H_2O on H_2O[b]	CO on CO	CO_2 on CO_2	CO on H_2O	CO_2 on H_2O	SO_2 on SO_2	H_2S on SO_2	CO_2 on SO_2	H_2 on H_2O:CH_3OH
5.....	1×10^{348}	1×10^{247}	3×10^{398}	3×10^{63}	6×10^{213}	2×10^{131}	3×10^{228}	4×10^{277}	2×10^{153}	3×10^{178}	7×10^{27}
10.....	1×10^{164}	1×10^{113}	2×10^{179}	8×10^{21}	7×10^{96}	6×10^{55}	2×10^{104}	2×10^{130}	5×10^{64}	2×10^{79}	5×10^{3}
15.....	4×10^{102}	1×10^{69}	4×10^{119}	1×10^{8}	8×10^{57}	4×10^{30}	7×10^{62}	2×10^{80}	3×10^{36}	2×10^{46}	5×10^{-5}
20.....	1×10^{72}	5×10^{46}	6×10^{84}	1×10^{1}	3×10^{38}	1×10^{18}	1×10^{42}	2×10^{55}	3×10^{22}	5×10^{29}	5×10^{-9}
30.....	3×10^{41}	3×10^{24}	8×10^{49}	1×10^{-6}	9×10^{18}	2×10^{5}	3×10^{21}	2×10^{30}	2×10^{8}	1×10^{13}	...
40.....	1×10^{26}	2×10^{13}	3×10^{32}	3×10^{-9}	2×10^{9}	1×10^{-1}	1×10^{11}	5×10^{17}	2×10^{1}	7×10^{4}	...
50.....	9×10^{16}	5×10^{6}	1×10^{22}	...	3×10^{3}	2×10^{-5}	7×10^{4}	1×10^{10}	1×10^{-3}	8×10^{-1}	...
60.....	7×10^{10}	2×10^{2}	1×10^{15}	...	3×10^{-1}	6×10^{-8}	5×10^{0}	1×10^{5}	2×10^{-6}	4×10^{-4}	...
70.....	3×10^{6}	1×10^{-1}	1×10^{10}	...	5×10^{-4}	1×10^{-9}	6×10^{-3}	4×10^{1}	2×10^{-8}	2×10^{-6}	...
80.....	1×10^{3}	5×10^{-4}	2×10^{6}	...	4×10^{-6}	...	4×10^{-5}	8×10^{-2}	6×10^{-10}	3×10^{-8}	...
90.....	4×10^{0}	6×10^{-6}	3×10^{3}	...	1×10^{-7}	...	7×10^{-7}	7×10^{-4}	...	1×10^{-9}	...
100.....	4×10^{-2}	2×10^{-7}	1×10^{1}	...	5×10^{-9}	...	3×10^{-8}	1×10^{-5}	...	...	...
110.....	1×10^{-3}	1×10^{-8}	2×10^{-1}	...	...	...	2×10^{-9}	6×10^{-7}	...	...	...
130.....	2×10^{-6}	...	2×10^{-4}	...	...	...	...	5×10^{-9}	...	...	...
150.....	3×10^{-8}	...	1×10^{-6}	...	...	...	...	...	...	...	...

[a] Residence times (yr) calculated using $t = \nu_0^{-1} \exp(\Delta H_s/kT)$ and $(\Delta H_s/k)$ values in Table 2. Values used for ν_0 were CO (2.0×10^{12} s^{-1}), CO_2 (2.9×10^{12} s^{-1}), H_2O (2.0×10^{12} s^{-1}), SO_2 (2.4×10^{12} s^{-1}), H_2S (1.94×10^{12} s^{-1}), CH_3OH (2.2×10^{12} s^{-1}), NH_3 (3.45×10^{12} s^{-1}), and H_2 (7.5×10^{12} s^{-1}).
[b] Unannealed.

Iglesias 1977). Indeed, while the question is often raised as to whether certain inconsistencies in the interpretation of gas phase observations might be explained by condensation onto grains, the more fundamental question is "Why do we see any molecular species present in the gas phase in dense clouds at all?" Because of condensation effects, radio observations will generally underestimate the total column densities of material. This limitation is not restricted to specific molecules, but is potentially important for virtually all molecular species observed in the gas phase in dense clouds. Thus, an understanding of the gas-grain interaction bears directly on interstellar chemistry and interstellar cloud physics.

During the past decade, several hypothesis have been put forward to address how molecules may leave the grains and reenter the gas phase. Suggested mechanisms include interstellar ice grain "explosions" driven by the sudden release of chemical energy stored in the form of radicals (Greenberg & Yencha 1973; d'Hendecourt et al. 1982) triggered by grain-grain collisions (d'Hendecourt, Allamandola, & Greenberg 1985) or heavy cosmic rays (Leger, Jura, & Omont 1985; Schutte & Greenberg 1991). Turbulent eddies within a cloud may also circulate grains from cooler to warmer regions, thereby evaporating enough of the ice mantles to replenish the gas phase (Boland & de Jong 1982; Williams & Hartquist 1984). Lower, variable sticking efficiencies have also been considered (Jones & Williams 1985). A review of the various attempts to reconcile the amount of material seen in the gas phase with the expected depletion onto grains can be found in Brown & Charnley (1990).

In this section we show that the physical nature of the ice, in conjunction with the condensation-vaporization properties of each of the components within the ice, *must* be taken into account if one is to have any hope of correctly accounting for the observations of both the gas and solid phases in interstellar clouds. We will demonstrate that interstellar ices can exhibit a rich variety of behaviors depending on their temperature, composition, and history. In this regard, future models that attempt to explain the chemistry of dense molecular clouds should deal with the molecules in the ice mantles as rigorously as they now do for the same molecules in the gas phase. While this encompasses an area in which a great deal of observational, theoretical, and experimental work remains to be done, we will show that it represents an area in which a great deal of fundamental progress may be made.

4.1. *The Gas Phase Abundance of* CH_3OH *in Hot Cores*

Radio observations of CH_3OH in hot, dense cores often show methanol abundances that are not possible to explain solely in terms of gas phase, ion-molecule chemistry alone (see Menten et al. 1988 and Millar, Herbst, & Charnley 1991 for recent discussions). It has been suggested that the large methanol abundances observed may arise from the evaporation of CH_3OH-rich molecular ice mantles in these locations (cf. Tielens & Allamandola 1987; Brown 1990; Brown, Charnley, & Millar 1992). Recent infrared observations have shown that the ices in many dense clouds do contain large abundances of CH_3OH (Tielens & Allamandola 1987; Grim et al. 1991; Allamandola et al. 1992; Skinner et al. 1992). These observations, in conjunction with the findings of Blake et al. (1991) and the CH_3OH-CH_3OH binding energy presented here, indicate that substantial fractionation of methanol from other interstellar molecules *can* be expected to occur when interstellar ices are warmed.

Blake et al. (1991) demonstrated that amorphous H_2O:CH_3OH mixed molecular ices convert spontaneously to a type II clathrate structure when warmed to 120 K under vacuum if the methanol concentration of the starting ice is greater than 6%–7%. This methanol concentration exactly fits the expected stochiometry since type II clathrates contain only enough voids to accommodate a 7% concentration of large guest molecules. During this conversion the clathrate can also accommodate a concentration of up to 14% of smaller guest molecules like CO and CO_2. Methanol abundances of $>7\%$ that of H_2O cannot be supported by a well-ordered type II clathrate and the behavior of CH_3OH-rich ices during warming through 120 K differs substantially for ices on opposite sides of the 7% abundance value. Blake et al. discovered that when H_2O:CH_3OH ices containing more than 7% CH_3OH were warmed to 120 K, the ice still underwent a spontaneous phase transition to form crystals of type II H_2O:CH_3OH clathrate. These clathrate crystals contained 7% methanol. However, during the phase transition the excess CH_3OH, which was excluded from the clathrate structure, formed crystals of pure CH_3OH ice intermixed with the crystals of H_2O:CH_3OH clathrate. At this point the ice consisted of two mixed solid domains, crystals of type II H_2O:CH_3OH clathrate and crystals of pure CH_3OH. During this separation, volatile gases like CO and CO_2 were trapped in the smaller voids of the clathrate (a process that probably continues up to an abundance of $\sim 14\%$).

A glance at the relative binding energies of H_2O on H_2O and CH_3OH on CH_3OH in Table 2 and the temperature-dependent residence times of these molecules in Table 3 shows that at 120–130 K the sublimation of the pure CH_3OH crystals will proceed 100–1000 times faster than that of the H_2O forming the skeleton of the type II clathrate. Indeed, Blake et al. (1991) observed the pure methanol ice crystals that formed during the enclathration to rapidly sublime away at 120 K. In contrast to the pure CH_3OH, more volatile species like CO and CO_2 were observed to be efficiently trapped in the clathrate and were only freed when the H_2O in the clathrate sublimed (see Blake et al. 1991 for an example with CO_2). Thus, *immediately following the formation of a type II clathrate at about 120* K *from an* H_2O*-rich ice containing more than* 7% CH_3OH, *there is a period during which the ice ejects methanol and only methanol into the gas phase. Furthermore, provided their abundance does not exceed* $\sim 14\%$ *that of the* H_2O, *more volatile materials like* CO *and* CO_2 *will not be given off during this transition since they are efficiently trapped in the* H_2O:CH_3OH *clathrate.* Less volatile species (like H_2O) will not be given off as quickly because the temperature is not high enough (Table 3).

As mentioned earlier, methanol has been identified in interstellar ices through the detection of a number of solid state absorption bands in the infrared. While the exact abundance of CH_3OH relative to H_2O in these ices is the subject of some controversy, in virtually all cases it is sufficiently high ($>5\%$) that it is expected that a type II clathrate will form when the ices are warmed to 120 K. The concentrations of all other known ice species lie below the 14% level relative to H_2O. As a result, interstellar ice grains of typical composition, when warmed above 120 K, should selectively eject any CH_3OH they contain above the 7% level while retaining the other volatile species present.

The physical behavior and sublimation properties of CH_3OH*-containing,* H_2O*-rich ices produce chemical differentiations that*

may offer a natural explanation for the high gas phase methanol abundances and molecular chemistry detected in hot molecular cores associated with star-forming regions. For example, the Orion-KL nebula contains two hot cores, one of which, the Compact Ridge ($n_H \sim 10^6$ cm^{-3}, $T_{gas} \sim$ 80–150 K; Genzel & Stutzki 1989), shows gas phase methanol abundances two to three orders of magnitude greater than can be explained by simple gas phase chemistry models (cf. Menten et al. 1988), but contains relatively little gas phase ammonia. Unlike the methanol, the ammonia abundance in these warmer regions appears to be consistent with gas phase ion-molecule reactions alone. In contrast, the second hot core in the Orion-KL nebula, the Orion Hot Core ($n_H > 10^7$ cm^{-3}, $T_{gas} \sim$ 200–300 K, $T_{dust} \sim$ 150 K; cf. Wynn-Williams et al. 1984; Genzel & Stutzki 1989), is denser and hotter and contains large quantities of gas phase NH_3 which can only have been introduced by grain processes like grain surface chemistry and evaporation. Charnley, Tielens, & Millar (1992) demonstrated that the differences between these two cores can be explained if species-specific sublimation occurs in selected regions of the cloud complex and suggested some sort of differentiation has occurred during the evaporation of the grain mantles. Given the clathrate expulsion process described above, the observations could be understood in the following terms. The Hot Core is sufficiently dense and hot that its grains will have been heated enough to have released their excess methanol, followed shortly thereafter by the release of all the other ice components (including NH_3) as the H_2O sublimed. The influence of the excess CH_3OH on the gas phase chemistry disappeared in the few $\times 10^4$ yr following the sublimation of the entire ice mantle due to ion-molecule reactions. The slower neutral-neutral chemistry associated with NH_3, however, has yet to deplete all the available ammonia and continues to the present. In contrast, the less dense and cooler Compact Ridge may contain ices that have only recently been warmed enough to have undergone the expulsion of excess CH_3OH during clathrate formation, but not to have appreciably evaporated the H_2O ice and its host volatiles (including NH_3). This would explain the observed high abundance of CH_3OH and lack of NH_3. A more detailed discussion of the effects these processes will have on the chemistry of the Orion-KL nebulae can be found in Charnley (1993).

Thus, *the selective sublimation of* CH_3OH *produced by the spontaneous vacuum enclathration of interstellar ices as they are warmed above* ~ 120 K *may provide a natural explanation for the dramatic variations in gas phase methanol abundances and the molecular differentiation observed in some hot core sources.*

4.2. H_2O:CH_3OH *Clathrates and Cometary Behavior*

The implications of H_2O:CH_3OH enclathration for cometary behavior have been discussed elsewhere (Blake et al. 1991). Since cometary ices are known to contain up to 6% methanol (Hoban et al. 1991), it is possible that cometary ices may undergo (or have already undergone) the vacuum enclathration process during warming above $\sim$120 K. As discussed above, this can have a significant effect on the partitioning of more volatile species like CO and CO_2 and can lead to the separation of a pure methanol phase from the clathrate.

The possibility of such a phase separation in comets is particularly intriguing since this process can turn a previously nonporous, amorphous H_2O-rich ice into an ice riddled by submicron pores. The importance of this process in terms of its effect on the thermal properties of comets and the transport of volatiles through their surface layers are obvious.

4.3. *The Depletion of Gas Phase* CO *in Cool Dense Cloud Cores*

It is apparent from the binding energies and residence times given in Tables 2 and 3 that many of the molecules in dense molecular clouds will be significantly depleted from the gas phase onto grain mantles. As already pointed out, this will lead to substantial underestimates of the true column densities of each species if the determinations are based solely on gas phase measurements. The amount by which the total column density will be underestimated will depend on the volatility of the molecule under consideration and the local cloud temperature and density. Even for the case of one of the most volatile molecules studied by radio astronomers, namely CO, depletion from the gas phase by condensation on grains is commonly observed (cf. Tielens et al. 1991; van Dishoeck et al. 1992a).

Using the binding energies listed in Table 2, it is possible to model these effects, thus providing for better estimates of the physical parameters of the clouds being studied. The fraction of a molecular species that is in the gas phase relative to the solid phase can be estimated simply by comparing (1) the time it takes the molecule in the gas phase to travel the mean free path length between dust grains with (2) the residence time of the molecule on the grain after it collides and sticks. The residence time on the grain is given by $t_s = \nu_0^{-1} \exp(\Delta H_s/kT_d)$, where all the variables are as defined previously and T_d is the temperature of the dust grain. The time it takes a molecule to travel one mean free path length in the gas phase is $t_g = 1/\nu_{rms} = (1/\pi n d^2 2^{1/2})/(2kT_g/m_g)^{1/2}$, where n is the number density of dust grains, d is the diameter of the dust grains, k is Boltzmann's constant, T_g is the temperature of the gas, and m_g is the mass of the molecule. Dividing the equation for the residence time on the grain by the equation for the free flight time yields the relative proportion, η, of the molecular species that should be found in the solid versus gas phase assuming only thermal processes are involved, namely

$$\eta = (2\pi n d^2/\nu_0)(kT_g/m_g)^{1/2} \exp(\Delta H_s/kT_d) . \quad (4)$$

While the temperature of the gas need not be the same as that of the dust, the density of most dense molecular clouds is sufficient to ensure that the two temperatures are very similar. As a result, the ratio of material in the solid to gas phase for any given molecule is expected to behave functionally as $T^{1/2}\, e^{1/T}$ and will scale linearly with the dust density. At the temperatures characteristic of dense molecular clouds (10–50 K), the exponential term dominates the behavior.

From the CO-CO binding energy found in Table 2, and the resulting residence times given in Table 3, it is apparent that, under certain conditions, CO in dense molecular clouds may remain in the solid phase over significant time scales. As an example, consider a crude molecular cloud model for NGC 2024 that contains both refractory dust and volatile components. For the sake of argument, we will define the refractory component to be those materials that are not expected to vaporize at temperatures above 200 K (i.e., silicates, carbon particles, etc.) and the volatile component to be all those materials that are expected to enter the gas phase at temperatures between 10 and 200 K (i.e., H_2O, CH_3OH, NH_3, CO, CO_2, etc.). Furthermore, assume the volatiles and refractories have a relative ratio by mass of 100 to 1 and that the general cloud medium has a temperature of 40 K and a density of 10^6 H atoms cm^{-3}. Embedded within the general cloud medium are cold dense cores in which the temperature drops to 20 K and the density increases to 10^8 H atoms cm^{-3}. (These particu-

lar values were chosen as they are similar to those inferred for NGC 2024 [cf. Mauersberger et al. 1992; Mezger et al. 1992]). If we assume the average dust grain is 0.1 μm in diameter and that the volatile mass is dominated by hydrogen, these values correspond to a density of dust particles of $\sim 2 \times 10^{-6}$ particles cm^{-3} in the general cloud medium and $\sim 2 \times 10^{-4}$ particles cm^{-3} in the cold cores.

The time it takes a CO molecule to travel one mean free path under these conditions is about 2300 yr in the general cloud medium and 33 yr in the cold cores. This compares to grain surface residence times of 3×10^{-9} and 1×10^{1} yr, respectively, for these two environments if the CO is freezing onto CO (Tables 3 and 4). (Corresponding times for CO sticking to H_2O-rich ices are not considered because the spectral profile of CO ices in dense molecular clouds indicates that while some CO is frozen in solid H_2O, most is frozen into nonpolar matrices [probably not pure CO; cf. Sandford et al. 1988; Tielens et al. 1991]). These result in ice-to-gas ratios of 1.3×10^{-12} and 3×10^{-1} for the general cloud and cores, respectively. Thus, CO under these conditions is expected to be almost entirely in the gas phase in the general cloud medium but should show measurable depletion in the cold cores (Table 4). In the case of CO, these predictions are in reasonable agreement with the observed gas phase CO depletions measured toward dense cores, which typically fall in the range of 1%–10% (cf. Tielens et al. 1991). This implies that most of the detected solid CO exists in the dense cores. Thus, to first order, *it appears that the depletion of* CO *in dense molecular clouds can be understood entirely in terms of its thermal condensation and sublimation properties.*

4.4. *The Depletion of Gas Phase* NH_3 *in Cool Dense Cloud Cores*

From the NH_3-NH_3 binding energy in Table 2 and the resulting residence times given in Table 3, it is apparent that ammonia should be severely depleted onto grains in dense molecular clouds. As with CO, an estimate of the extent of NH_3 depletion based on thermal effects alone can be made using equation (4). For the "model" interstellar cloud discussed in § 4.3, the time it takes an NH_3 molecule to travel its mean free path to collision with a dust grain is about 1800 yr in the general cloud medium and 25 yr in the dense cold cores. This compares with grain surface residence times of 2×10^{13} and 5×10^{46} yr, respectively, for these two environments (Tables 3 and 4). These result in an ice to gas ratio of about 1×10^{10} for NH_3 in the general cloud medium and 2×10^{45} in the cold core, i.e., *all* the NH_3 should be in the ice in both environments of NGC 2024! Even if we consider more typical, less dense clouds ($T = 30$ K, $n = 10^4$ cm^{-3} in the general cloud; $T = 20$ K, $n = 10^6$ cm^{-3} in the cores), these ratios only drop by factors of about 100. The observation of gas phase NH_3 in the face of these values raises several important issues.

Table 4 provides a quick summary of the expected depletions of CO and NH_3 in our hypothetical dense molecular cloud. It is clear that, in the absence of other than thermal effects, the *vast* majority of NH_3 in dense clouds must reside on the grains and *not* in the gas phase. Indeed, as stated earlier, *the real question is not whether there may be observable effects due to the condensation of* NH_3 *onto dust grains in dense clouds, but is instead why do we see any gas phase* NH_3 *in these clouds at all!* This dilemma is probably related to a second one, namely that the calculated relative depletion of ammonia between the cold core environment and that of the general cloud ($> 10^{35}$) is enormous compared to the relative depletions actually measured (on the order of 10^2–10^3 in NGC 2024; cf. Mauersberger et al. 1992). Both of these points represent serious issues that require further consideration.

We first consider the question of why the observed depletion of NH_3 in the cold cores is only a factor of 10^2–10^3 that of the general cloud medium when the thermal properties of NH_3 would suggest much larger values are appropriate. The observed relative depletion factor can be understood solely in terms of the free flight times of the NH_3 molecules before they hit and stick to a grain. At temperatures of 40 K and below, the residence time of NH_3 on a dust grain is greater than 10^{13} yr (Table 3). This timescale is effectively infinite for both the cores and the general cloud medium since typical dense molecular clouds only last for 10^7–10^8 yr. Thus, from a strictly thermal point of view, the gas phase ammonia can only be observed for one free flight time before it is condensed out for the remainder of the lifetime of the cloud or until the grains are warmed above 150 K. As a result, all other factors being equal, *the ratio of the depletion factor of* NH_3 *between the cold cores and the general cloud should scale directly with its free flight time, i.e.,*

TABLE 4

RESIDENCE TIMES (yr), FLIGHT TIMES (yr), AND DEPLETION FACTORS FOR CO AND NH_3 IN INTERSTELLAR CLOUDS

	CO					NH_3				
		General Cloud Medium[a]		Cold Cores[a]			General Cloud Medium		Cold Cores	
T (K)	Grain Surface Residence Time	Free Flight Time	Depletion Factor	Free Flight Time	Depletion Factor	Grain Surface Residence Time	Free Flight Time	Depletion Factor	Free Flight Time	Depletion Factor
10.....	8×10^{21}	4.6×10^{3}	1.7×10^{18}	4.6×10^{1}	1.7×10^{20}	1×10^{113}	3.6×10^{3}	2.8×10^{109}	3.6×10^{1}	2.8×10^{111}
20.....	1×10^{1}	3.3×10^{3}	3.0×10^{-3}	3.3×10^{1}	3.0×10^{-1}	5×10^{46}	2.5×10^{3}	2.0×10^{43}	2.5×10^{1}	2.0×10^{45}
30.....	1×10^{-6}	2.7×10^{3}	3.7×10^{-10}	2.7×10^{1}	3.7×10^{-8}	3×10^{24}	2.1×10^{3}	1.4×10^{21}	2.1×10^{1}	1.4×10^{23}
40.....	3×10^{-9}	2.3×10^{3}	1.3×10^{-12}	2.3×10^{1}	1.3×10^{-10}	2×10^{13}	1.8×10^{3}	1.1×10^{10}	1.8×10^{1}	1.1×10^{12}
60.....	...	1.9×10^{3}	...	1.9×10^{1}	...	2×10^{2}	1.5×10^{3}	1.3×10^{-1}	1.5×10^{1}	1.3×10^{1}
80.....	...	1.6×10^{3}	...	1.6×10^{1}	...	5×10^{-4}	1.3×10^{3}	3.9×10^{-7}	1.3×10^{1}	3.9×10^{-5}
100.....	...	1.5×10^{3}	...	1.5×10^{1}	...	2×10^{-7}	1.1×10^{3}	1.8×10^{-10}	1.1×10^{1}	1.8×10^{-8}

[a] Using the surface binding energy for CO on CO. Residence times and corresponding depletions for CO on H_2O are considerably larger (see Tables 2 and 3). For the general cloud, $n_H = 10^6$ cm^{-3}; for the cold cores $n_H = 10^8$ cm^{-3} (see § 4.3 for details). The underscored lines indicate the values associated with the typical temperature for each region.

with the grain density. The relative core–to–general cloud depletion is 10^2–10^3 because that is the difference in the dust densities of these two environments. (Note that the same statement is *not* true for CO, since the surface binding energy and residence times of this molecule on interstellar grains is considerably lower and CO can reenter the gas phase by normal sublimation on time scales smaller than the age of typical clouds [see Table 4]).

While this argument provides a simple explanation for the *relative* depletions of NH_3 between the general cloud and the cores, it does not answer the question of why there is a measurable amount of ammonia in the gas phase at all, i.e., why the *absolute* depletions are not as large as expected solely on the basis of thermal considerations (>99.99+% depletion onto the dust grains in virtually *all* dense cloud environments). As pointed out earlier, the presence of gas phase NH_3 in clouds may be the result of any of a number of physical processes that remove volatiles from the ices and return them to the gas phase. We next explore one additional possibility, namely that NH_3 is created directly in the gas phase at sufficient rate to balance losses by condensation.

It is plausible that N_2 is continuously recycled between the dust and gas phases by thermal evaporation in a manner similar to that described for CO above. N^+ produced by reaction of He^+ with the gas phase N_2 molecules can drive the formation of NH_3 via the reaction sequence $H_2 + N^+ \rightarrow H + NH^+$; $H_2 + NH^+ \rightarrow H + NH_2^+$; $H_2 + NH_2^+ \rightarrow H + NH_3^+$; $H_2 + NH_3^+ \rightarrow H + NH_4^+$; $e^- + NH_4^+ \rightarrow H + NH_3$, $H_2 + NH_2$ (see Herbst 1987 for a general discussion). This process may also result in the production of some N_2H^+ (S. B. Charnley, private communication), a species recently detected in the vicinity of one of the NGC 2024 cores (van Dishoeck et al. 1992b). It is conceivable that NH_3 made by this process could, under some circumstances, sufficiently balance the local losses due to condensation and a small gas phase NH_3 component could be continuously present. It seems unlikely, however, that this would be true in the general case. This process would ultimately be limited by the depletion of the available N_2, although the timescales for complete nitrogen depletion are probably greater than those of the existence of the cores themselves. Earlier models which included grain processes suggested that much of the observed ammonia may be produced via gas-grain chemistry (cf. d'Hendecourt et al. 1985; Brown & Charnley 1990; Nejad et al. 1990). The development of a model including all these possibilities would give much needed insight into N chemistry in molecular clouds.

Finally, it should be pointed out that depletions of gas phase NH_3 in dense molecular clouds may help explain a number of apparent "puzzles" associated with radio observations of this molecule. For instance, virial cloud masses derived from NH_3 gas phase observations are often much smaller than those based on observations of the dust continuum (cf. Mauersberger 1992), the NH_3 lines are often much narrower than those of CO (cf. Mundy et al. 1990; Mauersberger et al. 1992), the ammonia gas phase abundance often does not match the dust continuum (cf. Mundy et al. 1990), and the abundance of NH_3 relative to other molecules rarely matches that expected on the basis of simple gas phase production models (cf. Rawlings et al. 1992). Numerous authors have suggested that some or all of these discrepancies may be the result of the NH_3 being depleted from the gas phase by condensation onto grains, but most of these suggestions have been cast in very general terms and have not been rigorously pursued.

The observation that the distribution of gas phase NH_3 often does not match that of the dust continuum (cf. Mundy et al. 1990) is easily explained by condensation effects. The ratio of gas phase NH_3 to continuum dust emission will drop substantially wherever condensation occurs, both because ammonia is lost from the gas phase and because the condensed ammonia will then contribute to the dust continuum. The observation that NH_3 lines are often much narrower than those of CO in dense clouds (cf. Mundy et al. 1990; Mauersberger et al. 1992) can be understood in terms of the freezing out of NH_3 in cloud components with specific velocities, components in which the more volatile CO is not depleted from the gas phase. This point is explored in some detail in a paper by Rawlings et al. (1992). Using a slightly different formalism than presented here, they demonstrate that the narrower NH_3 lines can be reproduced when the condensation of gas phase ammonia is considered. Similarly, a depletion of NH_3 onto grains could explain why the virial cloud masses based on NH_3 gas phase observations often yield smaller values than those based on observations of the dust continuum (cf. Mauersberger et al. 1992), both because the depletion of NH_3 results in a lower computed column density of material and because the narrower lines imply a lower velocity dispersion. Condensation effects may also contribute to the fact that the distribution of gas phase CO is often observed to be more extended than that of NH_3 (cf. Myers 1983). Since the depletion of NH_3 onto grains will be substantially more severe than that of CO in all dense cloud environments, gas phase CO would be expected to have a wider distribution than gas phase NH_3 *independent* of other chemical effects (of course there is a second major effect here as well, namely that gaseous NH_3 must be at higher densities [$\sim 10^4$ cm^{-3}] than CO [10^2–10^3 cm^{-3}] if it is to be seen using radio techniques). These considerations demonstrate that a serious accounting of condensation and sublimation effects in interstellar chemistry models should prove to be very useful and that a great deal of progress in our understanding of dense molecular clouds is possible in this area. The binding energies presented here should help make this progress considerably more quantitative.

In summary, condensation and sublimation processes will effect the overall chemical composition of interstellar clouds in several ways. First, at higher densities ($n_H > 10^4$ cm^{-3}) the accretion time for most gases is less than the timescale needed for chemical steady state to be achieved ($\sim 10^7$ yr) and accretion dominates the chemistry by removing reactants from the gas. In addition, accretion processes will determine what species are on grain surfaces and will thus control the products created by gas-grain reactions (cf. Brown & Charnley 1990). The binding energies given in Table 2 provide a useful quantitative tool for modeling the condensation and sublimation of molecular species in dense clouds and should be used to expand the capabilities of interstellar chemistry models. Comparisons of accretion and sublimation rates will help determine the direction in which molecular species move during cloud evolution.

5. CONCLUSIONS

In an extension of previously reported work on ice systems containing H_2O, CO, CO_2, SO_2, H_2S, and H_2 ices (Sandford & Allamandola 1988, 1990a, 1993a, b), we present measurements of the surface binding energies and infrared spectral properties of ices containing CH_3OH and NH_3. These surface binding energies can be used to calculate the residence times of

the molecules on solid surfaces as a function of temperature, and thus represent a fundamental parameter needed for the thermal and chemical modeling of many astrophysical environments. Examples include interstellar ice mantles, comets, and the surfaces and atmospheres of many planets and satellites.

The surface binding energies of the CH_3OH-CH_3OH and NH_3-NH_3 ice systems were found to be 4235 ± 15 K and 3075 ± 25 K, respectively. A summary of all the binding energies we have determined to date is given in Table 2. These values indicate that *the molecules most commonly used in radio studies of dense clouds must be depleted from the gas phase by condensation onto cold dust grains. Thus, calculations derived from radio observations that ignore interactions between the gas and solid phases must, of necessity, underestimate the total column densities of material if they are based solely on gas phase measurements.* The extent of the depletion depends critically on the molecular species being considered and on the cloud temperature, density, thermal history, and chemistry, but for most species the depletion will be severe. The process(es) by which molecular species are removed from the ices and returned to the gas phase remains an important issue of concern.

In dense molecular clouds, the depletion is small for CO (typically $\lesssim 10\%$) and will generally be restricted to the colder, denser cores. The depletion of NH_3 should be severe in virtually *all* parts of molecular clouds. Since the residence time of NH_3 on dust grains is essentially "infinite" (when compared to cloud lifetimes) in all cloud environments, the relative depletions of NH_3 within a given cloud should scale primarily with the local dust density, although there are likely to be effects due to chemistry as well. These depletions may help explain the results of a number of radio studies of ammonia in dense clouds, including observations that (1) virial cloud masses derived from gas phase NH_3 are often smaller than those based on observations of the dust continuum, (2) CO often has velocity profiles that are much wider than those of NH_3, (3) the ammonia gas phase abundance often does not match the dust continuum, and (4) the abundance of NH_3 relative to other molecules rarely matches that expected on the basis of simple gas phase production models.

The proportion of a molecule in the ice versus gas phase can also be altered by solid state effects involving phase transitions during the warming of the ices and physical trapping of molecules within the matrix of a more refractory ice component. For example, when methanol-rich H_2O:CH_3OH ices similar to those seen in dense molecular clouds are warmed to 120 K they undergo a spontaneous phase transformation to a type II H_2O:CH_3OH clathrate (Blake et al. 1991). During this transition, any methanol that is present above the 7% level relative to H_2O is excluded and injected into the gas phase, while more volatile molecules like CO and CO_2 up to a relative abundance of $\sim 14\%$ relative to H_2O remain efficiently trapped in the clathrate. This process may explain small-scale abundance gradients in star-forming regions and suggests that they may be strongly connected to the local temperature.

As a result of these complications, it is incorrect to derive total column densities in dense molecular clouds based solely on radio maps of gas phase molecules. Similarly, chemical models that ignore the effects of grain accretion and sublimation are extremely unrealistic. Consideration of interactions with the solid state must be included. It is also clear that proper treatment of the affects of the grain-gas interaction will require that each of the ice components be individually studied in a variety of grain compositions and that each be separately considered in gas-grain chemistry models. In this respect, it will be necessary to treat the molecular components of ices individually, including all of their complexity, just as they already are in most gas phase models.

The authors would like to thank S. Charnley and J. Davidson for many useful and thought-provoking discussions during the preparation of this manuscript. This work was supported by NASA grants 199-52-12-04 (Exobiology) and 452-33-93-03 (origins of Solar Systems).

REFERENCES

Allamandola, L. J., Sandford, S. A., Tielens, A. G. G. M., & Herbst, T. M. 1992, ApJ, 399, 134
Allamandola, L. J., Sandford, S. A., & Valero, G. J. 1988, Icarus, 76, 225
Barthel, C., Gerbaux, X., & Hadni, A. 1970, Spectrochim. Acta, 26A, 1183
Blake, D., Allamandola, L., Sandford, S., Hudgins, D., & Freund, F. 1991, Science, 254, 548
Boland, W., & de Jong, T. 1982, ApJ, 261, 110
Brown, P. D. 1990, MNRAS, 243, 65
Brown, G. N., & Ziegler, W. T. 1980, Adv. Cryogenic Eng., 25, 622
Brown, P. D., & Charnley, S. B. 1990, MNRAS, 244, 432
Brown, P. D., Charnley, S. B., & Millar, T. J. 1992, in Chemistry and Spectroscopy of Interstellar Molecules, ed. N. Kaifu (Tokyo: Univ. Tokyo Press), 149
Charnley, S. B. 1993, in preparation
Charnley, S. B., Tielens, A. G. G. M., & Millar, T. J. 1992, ApJ, 399, L71
d'Hendecourt, L. B., & Allamandola, L. J. 1986, A&ASS, 64, 453
d'Hendecourt, L. B., Allamandola, L. J., Baas, F., & Greenberg, J. M. 1982, A&A, 109, L12
d'Hendecourt, L. B., Allamandola, L. J., & Greenberg, J. M. 1985, A&A, 152, 130
Eiroa, C., & Hodapp, K.-W. 1989, A&A, 210, 345
Frenkel, Z. 1924, Z. Phys., 26, 117
Fuller, G. A., & Myers, P. C. 1987, in Physical Processes in Interstellar Clouds, ed. G. E. Morfill & M. Scholer (Dordrecht: Reidel), 137
Genzel, R., & Stutzki, J. 1989, ARA&A, 27, 41
Greenberg, J. M. 1977, in Liège Astrophysical Symposium on the Spectra of Small Molecules (Liège: Univ. of Liège), 555
Greenberg, J. M., & Yencha, A. J. 1973, in Interstellar Dust and Related Topics, ed. J. M. Greenberg & H. C. van de Hulst (Dordrecht: Reidel), 369
Grim, R. J. A., Baas, F., Geballe, T. R., Greenberg, J. M., & Schutte, W. 1991, A&A, 243, 473
Hagen, W., Allamandola, L. J., & Greenberg, J. M. 1980, A&A, 86, L3
Herbst, E. 1987, in Interstellar Processes, ed. D. J. Hollenbach & H. A. Thronson, Jr. (Dordrecht: Reidel), 611
Hoban, S., Mumma, M., Reuter, D. C., DiSanti, M., Joyce, R. R., & Storrs, A. 1991, Icarus, 93, 122
Hollenbach, D., & Salpeter, E. E. 1970, J. Chem. Phys., 53, 79
Hudgins, D. M., Sandford, S. A., Allamandola, L. J., & Tielens, A. G. G. M. 1993, ApJS, in press
Iglesias, E. 1977, ApJ, 218, 697
Jones, K. 1973, in Comprehensive Inorganic Chemistry, ed. J. C. Bailar, H. J. Emeleus, R. Nyholm, & A. F. Trotman-Dickenson (Oxford: Pergamon Press), 209
Jones, A. P., & Williams, D. A. 1985, MNRAS, 217, 413
Knacke, R. F., McCorkle, S., Puetter, R. C., Erickson, E. F., & Kratschmer, W. 1982, ApJ, 260, 141
Landolt-Bornstein, H. H. 1978, in Numerical Data and Functional Relationships in Science and Technology, New Series, Group III, Crystal and Solid State Physics, 7, Crystal Structure Data of Inorganic Compounds, Part c1, Key Element N, ed. K.-H. Hellwege & A. M. Hellwege (New York: Springer-Verlag), 1
Langmuir, I. 1916, Phys. Rev., 8, 149
Leger, A., Jura, M., & Omont, A. 1985, A&A, 144, 147
Mauersberger, R., Wilson, T. L., Mezger, P. G., Gaume, R., & Johnston, K. J. 1992, A&A, 256, 640
Menten, K. M., Walmsley, C. M., Henkel, C., & Wilson, T. L. 1988, A&A, 198, 253
Mezger, P. G., Sievers, A. W., Haslam, C. G. T., Kreysa, E., Lemke, R., Mauersberger, R., & Wilson, T. L. 1992, A&A, 256, 631
Millar, T. J., Herbst, E., & Charnley, S. B. 1991, ApJ, 369, 147
Mundy, L. G., Wootten, H. A., & Wilking, B. A. 1990, ApJ, 352, 159
Meyers, P. C. 1983, ApJ, 270, 105
Nejad, L. A. M., Williams, D. A., & Charnley, S. B. 1990, MNRAS, 246, 183
Passchier, W. F. 1978, Ph.D. thesis, University of Leiden, 70
Rawlings, J. M. C., Hartquist, T. W., Menten, K. M., & Williams, D. A. 1992, MNRAS, 255, 471
Reuter, D. C. 1992, ApJ, 386, 330

Sandford, S. A., & Allamandola, L. J. 1988, Icarus, 76, 201
———. 1990a, Icarus, 87, 188
———. 1990b, ApJ, 355, 357
———. 1993a, Icarus, in press
———. 1993b, ApJ, 409, L65
Sandford, S. A., Allamandola, L. J., Tielens, A. G. G. M., Sellgren, K., Tapia, M., & Pendleton, Y. 1991, ApJ, 371, 607
Sandford, S. A., Allamandola, L. J., Tielens, A. G. G. M., & Valero, G. 1988, ApJ, 329, 498
Schudt, E., & Weitz, G. 1971, in Numerical Data and Functional Relationships in Science and Technology, New Series, Group III: Crystal and Solid State Physics, 5, Structure Data of Organic Crystals, Part a: $C \ldots C_{13}$, ed. K. H. Hellwege & A. M. Hellwege (New York: Springer-Verlag), 14
Schutte, W., Allamandola, L. J., & Sandford, S. A. 1993a, Science, 259, 1143
———. 1993b, Icarus, in press
Schutte, W., & Greenberg, J. M. 1991, A&A, 244, 190
Sill, G., Fink, U., & Ferraro, J. R. 1980, J. Opt. Soc. Amer., 70, 724
Skinner, C. L., Tielens, A. G. G. M., Barlow, M. J., & Justtanont, K. 1992, ApJ, 399, L79
Souers, P. C. 1986, Hydrogen Properties for Fusion Energy (Berkeley: Univ. of California Press)
Tielens, A. G. G. M., & Allamandola, L. J. 1987, in Physical Processes in Interstellar Clouds, ed. G. E. Morfill & M. Scholer (Dordrecht: Reidel), 333
Tielens, A. G. G. M., & Hagen, W. 1982, A&A, 114, 245
Tielens, A. G. G. M., Tokunaga, A. T., Geballe, T. R., & Baas, F. 1991, ApJ, 281, 181
van Dishoeck, E. F., Glassgold, A. E., Guelin, M., Jaffe, D. T., Neufeld, D. A., Tielens, A. G. G. M., & Walmsley, C. M. 1992a, in IAU Symp. 150, Astrochemistry of Cosmic Phenomena, ed. P. D. Singh (Dordrecht: Kluwer), 285
van Dishoeck, E. F., Phillips, T. G., Keene, J., & Blake, G. A. 1992b, A&A, 261, L13
van de Hulst, H. C. 1949, Rech. Astron. Obs. Utrecht, 11, 1
Walmsley, C. M. 1989, in IAU Symp. 135, Interstellar Dust, ed. L. J. Allamandola & A. G. G. M. Tielens (Dordrecht: Kluwer) 263
Williams, D. A., & Hartquist, T. W. 1984, MNRAS, 210, 141
Wynn-Williams, C. G., Genzel, R., Becklin, E. E., & Downes, D. 1984, ApJ, 281, 172

Note added in proof.—An additional absorption band of CH_3OH ice near 4130 cm^{-1} (2.42 μm) has recently been detected in the spectrum of WL 5 (S. A. Sandford & L. J. Allamandola, Science, in press [1993]), an object deeply embedded in the ρ Oph dense cloud complex. More surprisingly, the same spectrum also contains an absorption band due to large quantities of solid H_2 trapped within the H_2O ices along the same line of sight. Current estimates indicate that as much as 30% (by number) of the ice could be H_2 trapped in H_2O. This represents the ultimate example of the depletion of molecular species onto interstellar grains.